

An Automated Sleep Staging Method with EEG-based Sleep Structure Computation

Ruixiang Liao (21051217@hdu.edu.cn)

Zhuoyue Honors College, Hangzhou Dianzi University
Hangzhou, 310018 China

Li Zhu (zhuli@hdu.edu.cn)

School of Computer Science, Hangzhou Dianzi University
Hangzhou, 310018 China

Wanzeng Kong (kongwanzeng@hdu.edu.cn)

School of Computer Science, Hangzhou Dianzi University
Hangzhou, 310018 China

Zhengyi Wang (21051228@hdu.edu.cn)

School of Computer Science, Hangzhou Dianzi University
Hangzhou, 310018 China

Abstract

Sleep staging serves as the foundation for sleep assessment and disease diagnosis, constituting a crucial aspect of sleep research. The related work on automatic sleep staging has achieved numerous satisfactory outcomes. However, current research predominantly focuses on using sleep information as classification features, e.g. employing time-domain or frequency-domain measures as local features, and comprehensive brain network information across channels as global features, while overlooking the spontaneous regularities in brain activity. Simultaneously, brain microstates are considered closely linked to brain activity and can be used to investigate the regular variations in the overall brain potential. To explore the regular changes in the microstates of brain function during sleep stages based on electroencephalogram (EEG), especially the regular changes in sleep structure, we initially conduct microstate clustering, followed by characterizing the sleep structure of the participants based on these microstates. Subsequently, we integrate the sleep structure with traditional sleep information features and perform automatic sleep staging. Our experiments make the following contributions: (1) Being the first to introduce the use of sleep structure for automatic sleep staging. (2) When there are 7 or more than 7 microstate classes, the model performs well, and the best classification accuracy reaches 89.50%. (3) Proposing a sleep automatic staging model that integrates sleep structure and sleep information.

Keywords: automated sleep staging; EEG; microstate; sleep structure

Introduction

Sleep is an essential part of everyone's life and consists of multiple sleep cycles. The R&K Rules categorize sleep into wake (W), rapid eye movement (REM), and non-REM (NREM) phases. Within the NREM phase, there are additional subdivisions, including S1, S2, S3, and S4, based on the depth of sleep (Wolpert, 1969). In 2007, the American Academy of Sleep Medicine (AASM) made modifications to the staging criteria proposed by R&K. They combined S3 and S4 into a single stage and divided NREM into N1, N2, and N3 stages (Iber, Ancoli-Israel, Chesson, & Quan, 2007).

Sleep staging plays a crucial role in research areas like sleep quality assessment and the diagnosis of disorders, such as insomnia and obstructive sleep apnea (Wulff, Gatti, Wettstein, & Foster, 2010).

Sleep staging is characterized by temporal sequence, periodicity, and close association with brain activity. EEG signals, as real-time recorded scalp electrophysiological signals, are highly suitable for sleep staging. EEG is widely used in clinical settings for the detection of seizure (Chen, 2014), assessing of depression (Acharya et al., 2018), Alzheimer's classification (Kim & Kim, 2018) and bullying indices detection (Baltatzis, Bintsi, Apostolidis, & Hadjileontiadis, 2017). In the field of automated sleep staging, there are also several applications of EEG, such as frequency-domain with SVM (Lajnef et al., 2015), time-domain with SVM (Sharma, Goyal, Achuth, & Acharya, 2018), raw signal samples with CNN (Sors, Bonnet, Mirek, Vercueil, & Payen, 2018), and statistical and spectral features with LSTM-RNN (Michielli, Acharya, & Molinari, 2019). However, existing automated sleep staging methods based on EEG primarily rely on raw signal, frequency-domain, and time-domain information, without utilizing the inherent regularity and periodicity of sleep to construct sleep structure for automated sleep staging.

The construction of sleep structure presents some challenges. For instance, extracting a time-domain or frequency-domain feature from each sampling point for classification may easily lead to feature dimension explosion. Conversely, merging too many sampling points into a segment may cause the model to overlook some short but important temporal information. Microstate analysis, as a method that analyzes the global pattern of scalp potential topographies while considering each sampling point, is well-suited for constructing sleep structure. It utilizes the global field power (GFP) to perform clustering analysis on brain topographic maps at each

5773

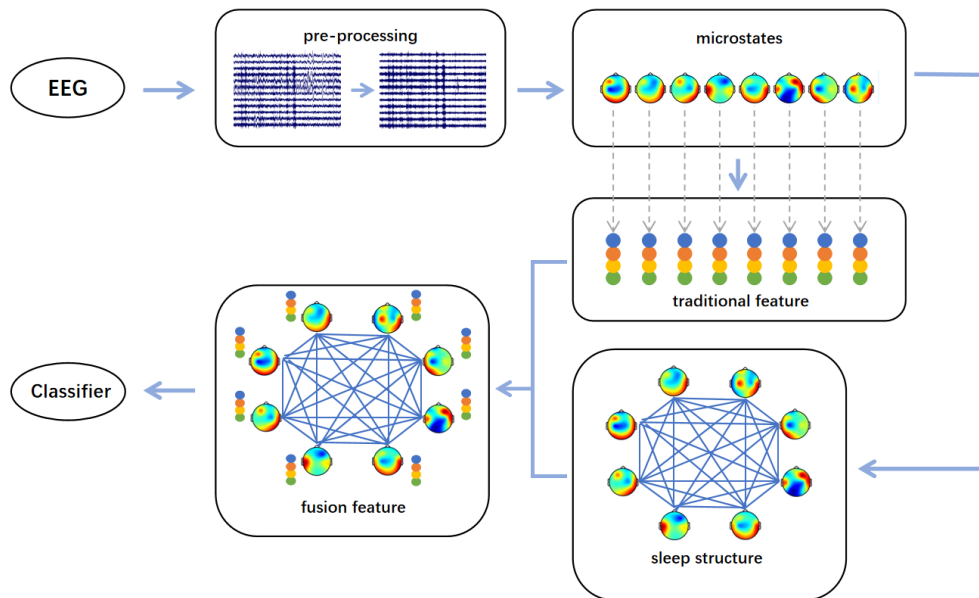


Figure 1: Framework of our proposed method.

moment. Therefore, based on the framework of microstates, this paper proposes a method for extracting structural changes during sleep staging phases.

To our best knowledge, this is the first work to extract the sleep structure information for sleep staging. We proposed a computation method based on EEG micro-state framework. Specifically, the sleep structure matrix is calculated like adjacency matrix in graph theory, e.g. each class is taking as a node and the transition relationship between classes is expressed as edges. The weight of an edge is determined by the frequency of transitions between two classes. After constructing the sleep structure, we analyze each microstate class independently. For each microstate class, the time domain and frequency domain features are extracted. Finally, the hybrid feature integrated by sleep structure matrix, time and frequency features is used for classification.

Method

Framework of Our Method

In this study, we proposed an automated sleep staging method with EEG-based sleep structure computation, as illustrated in Figure.1. This method comprises six modules:

Preprocessing module: This module applies filtering and downsampling operations to the raw EEG signal to remove unnecessary noise and reduce computational load.

Microstates module: Utilizing the Microstate analysis plugin from the EEGLAB toolbox (Poulsen, Pedroni, Langer, & Hansen, 2018), this module extracts scalp potential topographies and clusters them to obtain microstates from the EEG

signal.

Traditional Features module: Here, we extract zero-crossing rate, potential standard deviation, and Power Spectral Density (PSD) for each microstate category.

Sleep Structure module: In this module, we construct a sleep structure matrix based on the transition relationships between microstates.

Fusion Features module: Traditional features are integrated with sleep structure matrix to form fusion features. We concatenate traditional features onto the flattened one-dimensional sleep structure to form fusion features.

Classification module: We use the support vector machine (SVM) with the Gaussian kernel.

Dataset & Pre-processing

The data utilized in this paper is sourced from the publicly available CAP Sleep Database (Goldberger et al., 2000). It includes 16 healthy subjects without neurological disorders and drug-related issues. The number of EEG channels ranges from 3 to 12. Considering the completeness of sleep stages and channel coverage, we selected subjects (namely n3, n5, n10, and n11, respectively) who were recorded with 12 EEG channels, aged between 23 and 35 years old. Following the International 10–20 System, the bipolar electrodes were placed at Fp2-F4, F4-C4, C4-P4, P4-O2, F8-T4, T4-T6, Fp1-F3, F3-C3, C3-P3, P3-O1, F7-T3, and T3-T5, as shown in Figure 2. The data was sampled at a rate of 512 Hz. Each subject’s continuous recorded sleep EEG spanned approximately 9 hours, from 10:30 p.m. to 7:30 a.m. The sleep stages were

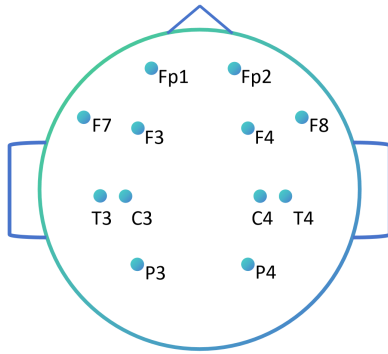


Figure 2: These 12 electrodes are used for EEG signal collection from subjects.

annotated by experts following the standard rules outlined by R&K every 30 seconds. Sleep is a cyclical process, with each cycle lasting approximately 90 to 110 minutes. Typically, humans undergo 4 to 5 sleep cycles per night.

In the pre-processing stage, we first conducted filtering to extract EEG signals within the 0.5–40Hz range. This includes six frequency bands: delta (0.5–4 Hz), theta (4–8 Hz), alpha (8–13 Hz), beta1 (13–22 Hz), beta2 (22–30 Hz), and gamma (30–40 Hz). Subsequently, to reduce computational load, we downsampled the data from 512Hz to 100Hz.

Sleep Structure Extraction-microstates

The global activity of brain can be characterized using the global field power (GFP), defined as the root of the mean of the squared potential differences between each electrode (i.e., $V_i(t)$) and the mean of instantaneous potentials across k electrodes (i.e., $V_{mean}(t)$) (Lehmann & Skrandies, 1980).

$$GFP = \sqrt{\left(\sum_i^k (V_i(t) - V_{mean}(t))^2 \right) / k} \quad (1)$$

Peaks in the GFP curve denote instances of maximum field intensity and optimal topographic signal-to-noise ratio. Within microstate analysis, the electric field topographies at these peaks in the GFP curve are regarded as distinct states of the EEG, with the signal’s progression viewed as a sequence of these states.

Studying microstates holds potential significance for understanding regular brain activity patterns. One possibility is that during certain brain activities, such as sleep, neurons emit electrical signals as a coordinated whole according to specific structured patterns, with close interconnections between individual neurons. This leads to the presence of a global pattern in the EEG signals recorded from the entire scalp. Based on this hypothesis, we propose a method for constructing sleep structures to facilitate automated sleep staging.

In the process of constructing the sleep structure, we integrated principles from graph theory. In graph theory, a graph

is a mathematical structure composed of nodes (vertices) and edges, used to describe relationships between objects. The weighted adjacency matrix serves as a representation of a graph, with its size being $n \times n$ (where n is the number of nodes in the graph). Each element of the matrix represents the connection between two nodes, typically the weight of the edge. In this study, we regard the entire sleep process as a directed graph, where each microstate class is considered as a node, and the number of transitions from one microstate to another serves as the weight of the directed edge. Thus, we construct the sleep structure matrix accordingly.

Time-domain and Frequency-domain Features

Time-domain analysis and frequency-domain analysis are two commonly used methods in EEG signal processing. The time domain refers to the process of analyzing signals along the time axis. The frequency domain refers to the process of analyzing the frequency content of signals. Sleep staging based on sleep structure is an analysis method independent of time-domain analysis and frequency-domain analysis. However, we also hope to combine traditional methods of extracting time-domain and frequency-domain features to construct sleep characteristics more comprehensively. In this study, we selected zero-crossing rate and standard deviation of raw EEG as two time-domain features, and PSD as a frequency-domain feature, to supplement the sleep structure.

Zero-crossing rate (ZCR) is a feature commonly used in signal processing to characterize the frequency of changes in the sign of a signal. It measures the rate at which a signal crosses the zero axis or changes its sign within a given time window.

Power spectral density (PSD) represents the power contained within specific frequency components of a signal. It quantifies the distribution of signal power as a function of frequency. It is often calculated using techniques such as the Fast Fourier Transform (FFT) or Welch’s method.

Classifier

We adopts SVM to classify different EEG sleep stages utilizing the Gaussian kernel function in the LIBSVM library (Chang & Lin, 2011). The One-against-one strategy was employed to accomplish multi-class classification, and the five fold cross validation is used for classifier training.

Results

Due to the distinct differences between the wakefulness (W) stage and other sleep stages, which are not the primary focus of automated sleep staging, we provides our discussion in this section with the experimental results of N1, N2, N3, and REM stages.

For a more in-depth analysis and a clearer presentation of sleep structure, we will extensively discuss the amount of microstates in each stage and visualize the sleep structure matrix which represents the transition status between microstates. We conducted classification experiments with the classes of microstate from 4 to 10. In addition, to test the model’s

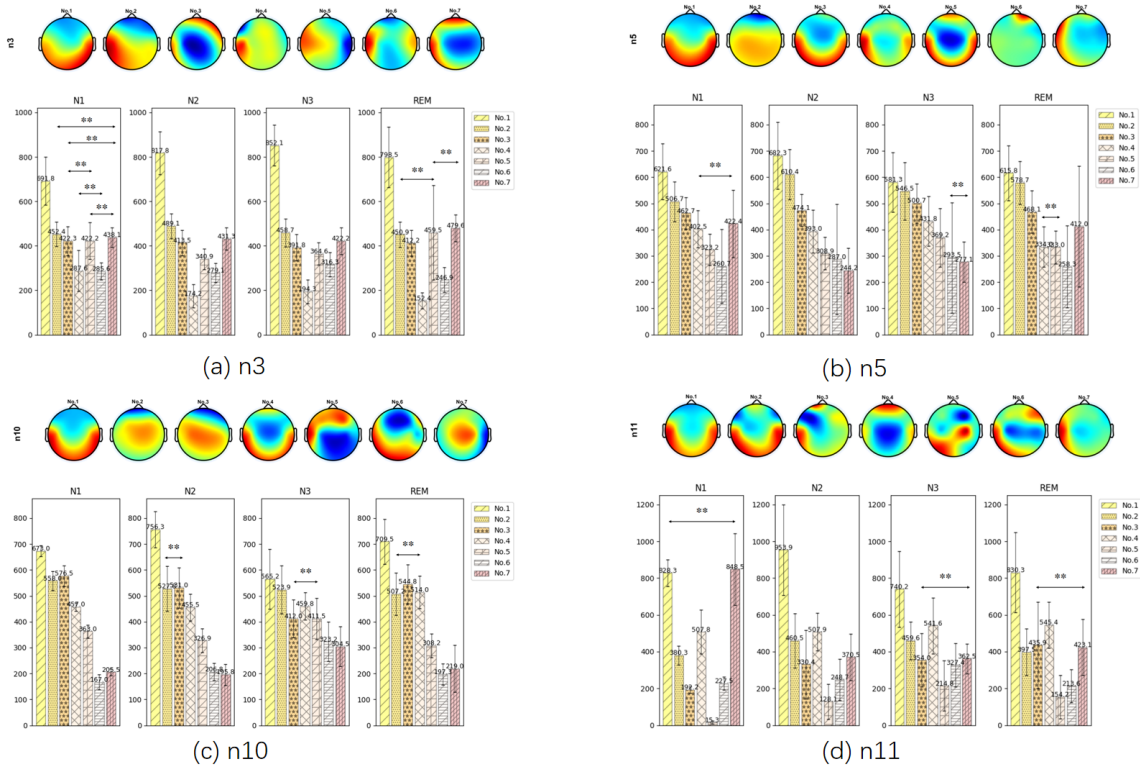


Figure 3: Result obtained from Topographical maps and the number of microstates. (a)-(d) stands for n3, n5, n10 and n11 respectively.

performance with fewer channels, we conducted classification experiments using electrodes from both the left and right hemispheres under the condition of a microstate number of 7 with 6 channels.

Average Amount of Each Microstate for Different Sleep Stages

For the subject n3 (as shown in Figure 3 (a)), the number of microstates during REM stage is extremely low for No. 4 microstate; whereas during N3 stage, No. 1 microstate has the highest count among all stages. Across all stages, No. 1 microstate consistently has the highest count within each stage. In the N1 stage, No. 2 and No. 7, No. 3 and No. 5, No. 3 and No. 7, No. 4 and No. 6, No. 5 and No. 7 show significant differences according to ANOVA test. In the REM stage, No. 2 and No. 5, No. 5 and No. 7 exhibit significant differences.

For subject n5 (as shown in Figure 3 (b)), there is generally a large variance in the count of each microstate. Significant differences in count are observed for No. 4 and No. 7 in the N1 stage, No. 6 and No. 7 in the N3 stage, and No. 4 and No. 5 in the REM stage.

For subject n10 (as shown in Figure 3 (c)), this participant is quite distinctive as it has very few samples labeled as N1, rendering significant analysis within N1 impossible. Significant differences in count are observed for No. 2 and No. 4 during REM, No. 2 and No. 3 during N2, and No. 3 and No.

5 during N3.

For subject n11 (as shown in Figure 3 (d)), there are a large number of occurrences of No.7 in its N1 stage, while the occurrences of No.5 are particularly few. Significant differences are observed for No. 1 and No. 7 during N1, No. 3 and No. 7 during N3, and No. 3 and No. 7 during REM.

Average Amount of Transitions between Microstates

The sleep structure matrices of the subjects are shown respectively in Figure 4. For n3, n5, and n10, it can be observed that the sleep matrices of N1 and N2 stages are very similar, which to some extent leads to difficulty in distinguishing between N1 and N2. The sleep matrices of all subjects during N3 stage are relatively flat, indicating inactive state transitions in the brain during N3 stage. The shape of the REM stage is similar to that of N1 and N2 stages, but there may be differences in the positions of the maximum values.

Classification Performance of Different Numbers of Microstates

From Table 1, the classification performance is relatively better under the 7 microstates circumstance for both n3 and n5. While for n10 and n11, it is the second highest and very close to the highest accuracy. In the process of microstate number ranging from 4 to 10, the accuracy generally shows an initial increase, approaching the peak at 7, and fluctuating to some extent between 7 and 10. The amounts of microstates exceed-

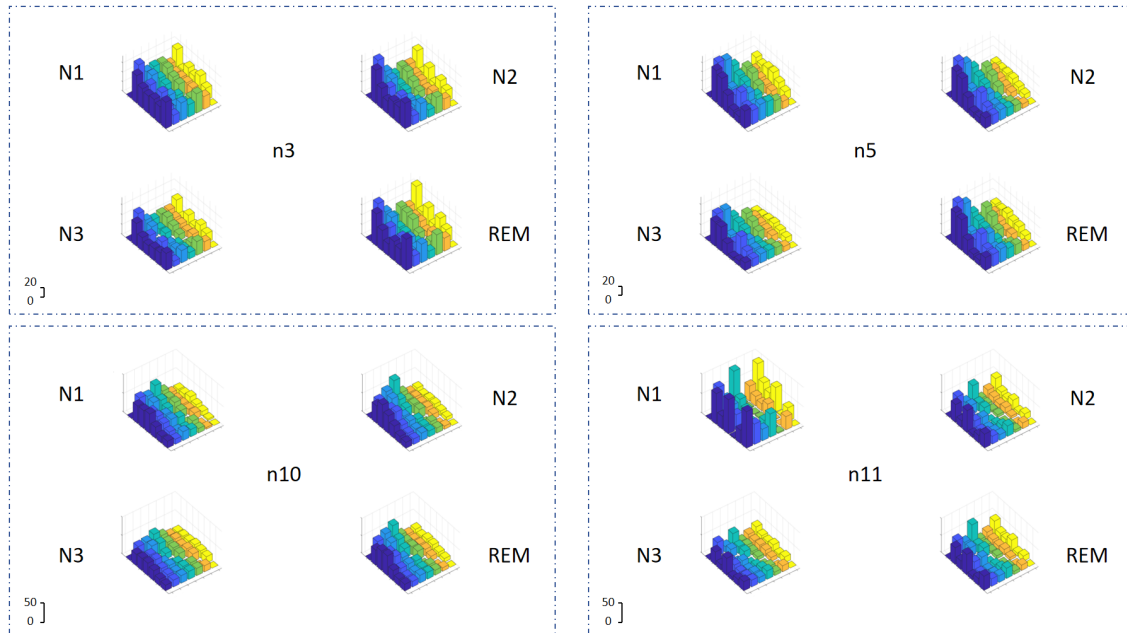


Figure 4: Sleep structure matrix based on the transition relationships between microstates, the height of the bars represents the average number of transitions between different microstates.

Table 1: The average accuracy of our model between different number(amount) of microstates(%).

Amount	n3	n5	n10	n11
4	86.78±0.30	85.80±0.42	86.20±0.51	83.22±0.47
5	88.04±0.42	85.97±0.33	86.91±0.23	84.69±0.52
6	88.80±0.31	86.67±0.60	87.88±0.52	84.81±0.38
7	89.50±0.12	86.93±0.29	89.40±0.22	87.40±0.44
8	88.02±0.21	86.28±0.55	88.52±0.29	86.17±0.34
9	88.28±0.37	86.58±0.58	88.73±0.25	87.51±0.38
10	88.66±0.30	86.63±0.24	89.41±0.42	83.38±0.29

Table 2: The average accuracy of our model with cerebral hemisphere channels(%).

Subject	right	left
n3	88.08±0.12	87.14±0.18
n5	85.26±0.11	85.92±0.12
n10	88.48±0.26	88.72±0.26
n11	87.52±0.20	86.76±0.25

ing 10 are not discussed in this paper due to limitations in the data: some individual subjects were unable to consistently cluster into 11 microstate classes.

Classification Performance of Cerebral Hemisphere EEG Signal

To test the model's performance with fewer channels, we conducted experiments using 6 channels from both the left and right hemispheres under the condition of a microstate number of 7. The experimental results are shown in Table 2. It can be observed that the model's performance decrease insignificantly compared to when using 12 channels. Additionally, the classification accuracy of the left and right hemispheres of the brain is similar, without significant hemispheric differences. Therefore, the used channels could be further decreased such as using half hemisphere signals for future practical applications.

Conclusions

In this paper, we propose a method for automatic sleep staging using sleep structure matrix computation. We use microstates to construct the sleep structure, then extract features based on each microstate. The sleep information is fused with the sleep structure to obtain fusion features for classification. We investigate the effects of sleep structure and different information on automatic sleep staging through experiments with a small number of channels and varying amounts of microstates. We obtain the following three points:

1. Constructing sleep structure using microstates is an effective approach.
2. As the amount of microstates used by the model increases, the accuracy gradually rises from 4 to 7 microstates and there is no clear upward or downward trend in accuracy from 7 to 10 microstates, but rather some fluctuation.
3. Sleep structure can be fused with sleep information to improve classification tasks.

Acknowledgments

This work was supported by Zhejiang Provincial Natural Science Foundation of China under Grant No. LQ24F020035 and the National Science Foundation of China under Grant No. 62301196, National Key Research and Development Program of China under Grant No. 2023YFE0114900; in part by the National Science Foundation of China under Grant U20B2074; in part by the Key Research and Development Project of Zhejiang Province under Grant No.2020C04009; and was also supported by Laboratory of Brain Machine Collaborative Intelligence of Zhejiang Province (2020E10010). Corresponding author: Li Zhu.

Furthermore, many thanks go to my family for their love. My parents have always been here to offer their support. I am also grateful for my grandpa's care and love in life. As he suffers from a stroke, I sincerely hope that the development of brain-computer interfaces can help alleviate his condition. Also, I want to express gratitude for my grandma's dedication to our family.

Once again, I thank all my family, teachers and friends for their support.

References

- Acharya, U. R., Oh, S. L., Hagiwara, Y., Tan, J. H., Adeli, H., & Subha, D. P. (2018). Automated eeg-based screening of depression using deep convolutional neural network. *Computer methods and programs in biomedicine*, 161, 103–113.
- Baltatzis, V., Bintsi, K.-M., Apostolidis, G. K., & Hadjileontiadis, L. J. (2017). Bullying incidences identification within an immersive environment using hd eeg-based analysis: A swarm decomposition and deep learning approach. *Scientific reports*, 7(1), 17292.
- Chang, C.-C., & Lin, C.-J. (2011). Libsvm: a library for support vector machines. *ACM transactions on intelligent systems and technology (TIST)*, 2(3), 1–27.
- Chen, G. (2014). Automatic eeg seizure detection using dual-tree complex wavelet-fourier features. *Expert Systems with Applications*, 41(5), 2391–2394.
- Goldberger, A. L., Amaral, L. A., Glass, L., Hausdorff, J. M., Ivanov, P. C., Mark, R. G., . . . Stanley, H. E. (2000). PhysioBank, physioToolkit, and physioNet: components of a new research resource for complex physiologic signals. *circulation*, 101(23), e215–e220.
- Iber, C., Ancoli-Israel, S., Chesson, A. L., & Quan, S. F. (2007). The new sleep scoring manual—the evidence behind the rules. *Journal of Clinical Sleep Medicine*, 3(02), 107–107.
- Kim, D., & Kim, K. (2018). Detection of early stage alzheimer's disease using eeg relative power with deep neural network. In *2018 40th annual international conference of the IEEE engineering in medicine and biology society (EMBC)* (pp. 352–355).
- Lajnef, T., Chaibi, S., Ruby, P., Aguera, P.-E., Eichenlaub, J.-B., Samet, M., . . . Jerbi, K. (2015). Learning machines and sleeping brains: automatic sleep stage classification using decision-tree multi-class support vector machines. *Journal of neuroscience methods*, 250, 94–105.
- Lehmann, D., & Skrandies, W. (1980). Reference-free identification of components of checkerboard-evoked multichannel potential fields. *Electroencephalography and clinical neurophysiology*, 48(6), 609–621.
- Michielli, N., Acharya, U. R., & Molinari, F. (2019). Cascaded lstm recurrent neural network for automated sleep stage classification using single-channel eeg signals. *Computers in biology and medicine*, 106, 71–81.
- Poulsen, A. T., Pedroni, A., Langer, N., & Hansen, L. K. (2018). Microstate eeglab toolbox: An introductory guide. *BioRxiv*, 289850.
- Sharma, M., Goyal, D., Achuth, P., & Acharya, U. R. (2018). An accurate sleep stages classification system using a new class of optimally time-frequency localized three-band wavelet filter bank. *Computers in biology and medicine*, 98, 58–75.

- Sors, A., Bonnet, S., Mirek, S., Vercueil, L., & Payen, J.-F. (2018). A convolutional neural network for sleep stage scoring from raw single-channel eeg. *Biomedical Signal Processing and Control*, *42*, 107–114.
- Wolpert, E. A. (1969). A manual of standardized terminology, techniques and scoring system for sleep stages of human subjects. *Archives of General Psychiatry*, *20*(2), 246–247.
- Wulff, K., Gatti, S., Wettstein, J. G., & Foster, R. G. (2010). Sleep and circadian rhythm disruption in psychiatric and neurodegenerative disease. *Nature Reviews Neuroscience*, *11*(8), 589–599.